Electronic Supplementary Material (ESI) for Physical Chemistry Chemical Physics.

Supporting Information for

Transport properties of nitrile and carbonate solutions of [P66614][NTf_2] ionic liquid, its thermal degradation and non-isothermal kinetics of decomposition

Ekaterina A. Arkhipova *[1], Anton S. Ivanov [1], Sergei S. Reshetko [1], Dmitry Yu. Aleshin [2], Konstantin I. Maslakov [1], Stepan Yu. Kupreenko [1] and Serguei V. Savilov [1]

[1] Department of Chemistry, Lomonosov Moscow State University, 1–3 Leninskiye Gory, Moscow 119991, Russia

[2] A. N. Nesmeyanov Institute of Organoelement Compounds, Russian Academy of Sciences, Vavilov str., 28, Moscow 119991, Russia

ekaterina.a.arkhipova@gmail.com

Table S1. Viscosity and dielectric constant of used chemicals.

Chemical	Abbreviation	CAS No.	Initial mass fraction purity	η, mPa·s	ε_r
acetonitrile	AN	75-05-8	≥ 99.9 %	0.3[1]	36[1]
propionitrile	PN	107-12-0	99.9 %	0.42[2]	25.9[3]
dimethyl carbonate	DMC	616-38-6	≥ 99.0 %	0.59[1]	3.1[1]
diethyl carbonate	DEC	105-58-8	≥ 99.0 %	0.75[1]	2.8[1]
trihexyl(tetradecyl)phosphonium bis(trifluoromethylsulfonyl)amide	[P66614][NTf_2]	460092-03-9	≥ 95.0 %	304[4]	–

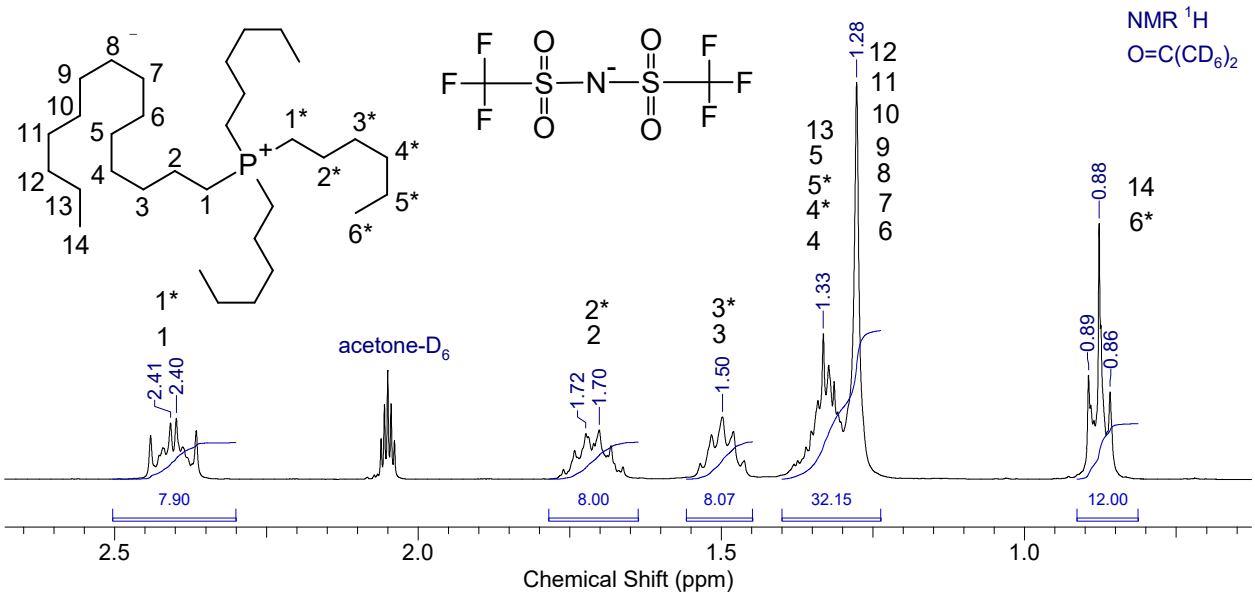

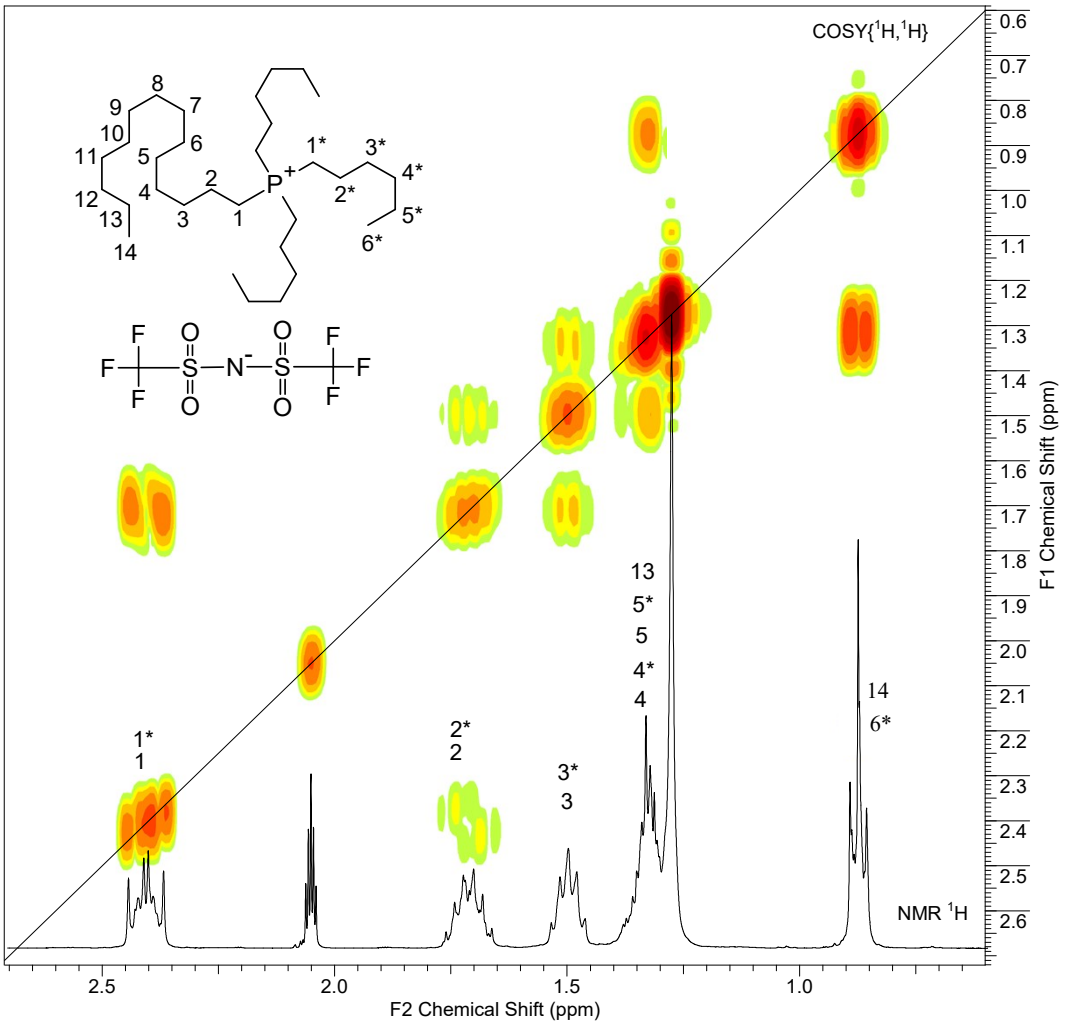

Figure S1. ^{1}H and COSY NMR spectra of [P66614][NTf$_2$].

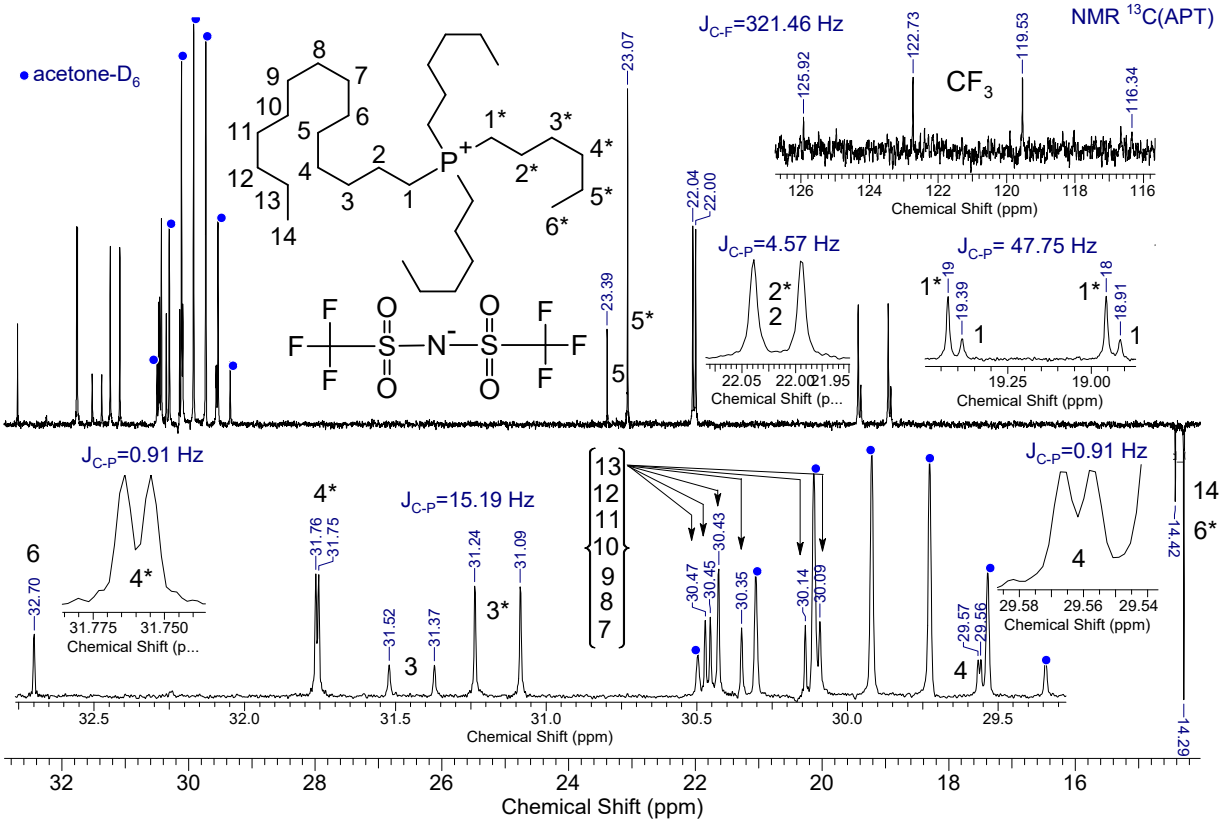

Figure S2. ^{13}C NMR (APT) spectrum of [P66614][NTf$_2$].

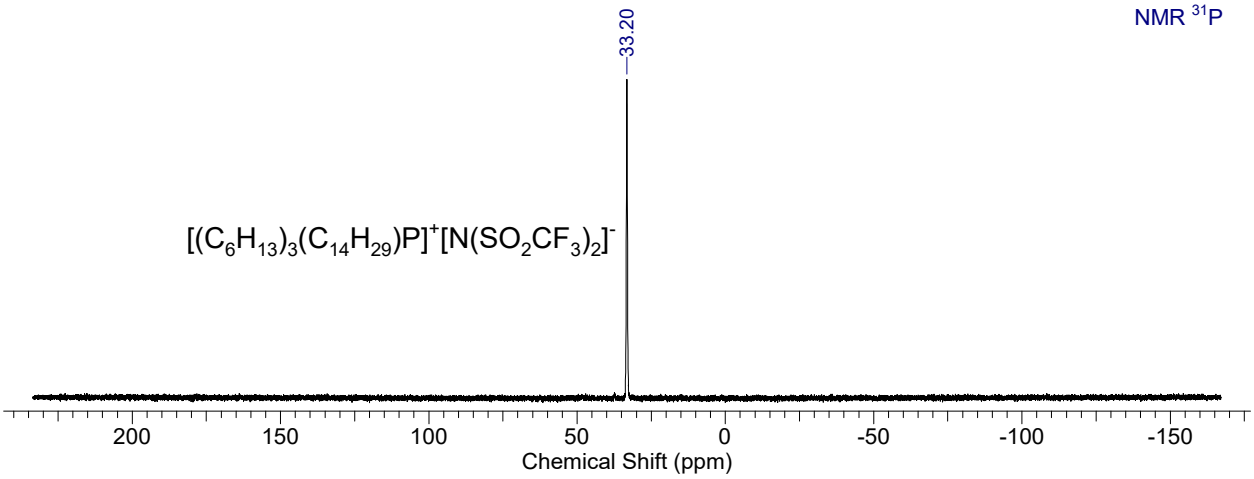

Figure S3. ^{31}P NMR spectrum of [P66614][NTf$_2$].

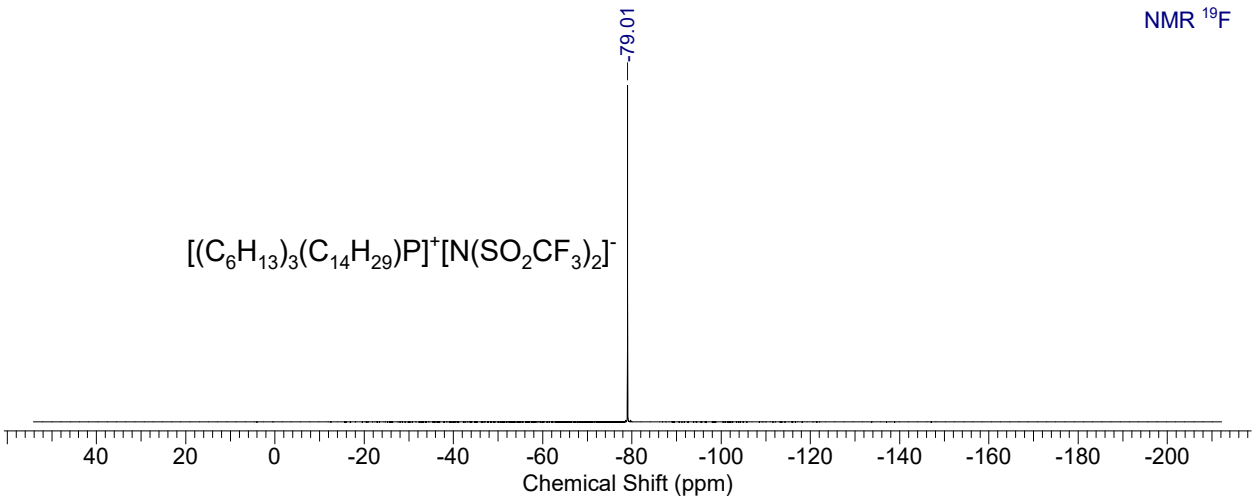

Figure S4. ^{19}F NMR spectrum of [P66614][NTf_2].

Table S2. Interpretation of ^{1}H, ^{13}C, ^{19}F and ^{31}P NMR signals.

NMR nucleus	Chemical shift/ ppm	Number of nuclei	Multiplicity of signal	Spin-spin coupling constant/ Hz	Interpretation
^{1}H	2.41	8	m.	-	1, 1*
	1.71	8	m.	-	2, 2*
	1.50	8	m.	-	3, 3*
	1.33	18	m.	-	4, 4*, 5, 5*, 13
	1.28	14	s.	-	6, 7, 8, 9, 10, 11, 12
	0.88	12	m.	-	6*, 14
^{13}C	120.83	1	q., ^{1}J (^{13}C-^{19}F)	321.46	CF_3
	32.70	1	s.	-	6
	31.76	3	d., ^{4}J (^{13}C-^{31}P)	0.91	4*
	31.45	1	d., ^{3}J (^{13}C-^{31}P)	15.19	3
	31.17	3	d., ^{3}J (^{13}C-^{31}P)	15.19	3*
	30.37	1	s.	-	7, 8, 9, 10, 11, 12, 13
	30.45	1	s.	-	
	30.43	2	s.	-	
	30.35	1	s.	-	
	30.14	1	s.	-	
	30.09	1	s.	-	
	29.57	1	d., ^{4}J (^{13}C-^{31}P)	0.91	4
	23.39	1	s.	-	5
	23.07	3	s.	-	5*
	22.02	4	d., ^{2}J (^{13}C-^{31}P)	4.57	2, 2*
	19.20	3	d., ^{1}J (^{13}C-^{31}P)	47.75	1*
	19.15	1	d., ^{1}J (^{13}C-^{31}P)	47.75	1
	14.42	1	s.	-	14
	14.29	3	s.	-	6*
^{19}F	-79.01	3	s.	-	CF_3
^{31}P	33.20	1	s.	-	$[P(C_6H_{13})_3(C_{14}H_{29})]^+$

Table S3. Electrical conductivities (σ) of [P66614][NTf_2] binary solutions in AN, PC, DMC and DEC as function of IL mole fraction (x_i) at T = 293 K measured in this work and calculated using the QSPR model.

AN			PN			DMC			DEC		
x_i	σ/ mS·cm^{-1}	σ_{QSPR}/ mS·cm^{-1}	x_i	σ/ mS·cm^{-1}	σ_{QSPR}/ mS·cm^{-1}	x_i	σ/ mS·cm^{-1}	σ_{QSPR}/ mS·cm^{-1}	x_i	σ/ mS·cm^{-1}	σ_{QSPR}/ mS·cm^{-1}
1.0000	0.07	0.47	1.0000	0.08	0.48	1.0000	0.06	0.47	1.0000	0.06	0.46
0.5586	0.30	0.69	0.6969	0.19	0.58	0.6265	0.16	0.55	0.6938	0.11	0.51
0.4075	0.60	0.95	0.5555	0.32	0.70	0.4594	0.29	0.68	0.5484	0.17	0.57
0.3102	1.07	1.38	0.4331	0.57	0.93	0.3598	0.47	0.84	0.4456	0.25	0.63
0.2502	1.75	2.00	0.3601	0.85	1.19	0.2857	0.70	1.05	0.3760	0.32	0.70
0.2113	2.45	2.64	0.2920	1.33	1.62	0.2474	0.88	1.21	0.3203	0.39	0.77
0.1805	3.30	3.41	0.2359	2.02	2.25	0.2157	1.06	1.37	0.2774	0.47	0.84
0.1580	4.11	4.14	0.1969	2.76	2.92	0.1891	1.22	1.52	0.2446	0.53	0.89
0.1393	4.96	4.92	0.1668	3.57	3.65	0.1591	1.39	1.67	0.2177	0.58	0.94
0.1241	5.82	5.71	0.1430	4.39	4.41	0.1396	1.50	1.77	0.1945	0.62	0.98
0.1118	6.65	6.45	0.1222	5.30	5.23	0.1215	1.56	1.83	0.1752	0.65	1.00
0.1012	7.41	7.14	0.1060	6.11	5.97	0.1034	1.59	1.86	0.1563	0.67	1.02
0.0926	8.15	7.82	0.0942	6.77	6.57	0.0880	1.55	1.82	0.1410	0.68	1.03
0.0842	8.94	8.53	0.0843	7.37	7.11	0.0791	1.50	1.77	0.1287	0.68	1.03
0.0779	9.56	9.10	0.0750	7.97	7.66	0.0697	1.40	1.68	0.1193	0.68	1.03
0.0724	10.07	9.57	0.0671	8.44	8.08	0.0616	1.29	1.58	0.1098	0.66	1.01
0.0680	10.46	9.92	0.0600	8.84	8.45	0.0550	1.16	1.47	0.1017	0.65	1.00
0.0637	10.90	10.32	0.0543	9.14	8.72	0.0498	1.07	1.38	0.0936	0.62	0.98
0.0601	11.27	10.65	0.0495	9.36	8.92	0.0453	0.99	1.31	0.0862	0.60	0.96
0.0563	11.66	11.01	0.0455	9.50	9.04	0.0411	0.90	1.23	0.0806	0.58	0.94
0.0534	11.94	11.26	0.0419	9.61	9.15	0.0375	0.82	1.15	0.0748	0.55	0.91
0.0501	12.29	11.58	0.0386	9.66	9.19	0.0336	0.72	1.07	0.0690	0.52	0.88

0.0472	12.57	11.84	0.0358	9.68	9.21	0.0304	0.64	0.99	0.0630	0.48	0.85
0.0444	12.84	12.08	0.0322	9.61	9.14	0.0264	0.54	0.90	0.0576	0.45	0.82
0.0418	13.07	12.29	0.0293	9.50	9.04	0.0233	0.45	0.82	0.0522	0.41	0.78
0.0389	13.37	12.56	0.0265	9.34	8.90	0.0213	0.40	0.77	0.0464	0.37	0.74
0.0359	13.45	12.64	0.0241	9.14	8.72	0.0193	0.35	0.73	0.0414	0.33	0.71
0.0334	13.53	12.71	0.0221	8.94	8.54	0.0174	0.30	0.68	0.0353	0.27	0.66
0.0309	13.53	12.71	0.0197	8.63	8.26				0.0300	0.22	0.61
0.0283	13.52	12.70	0.0176	8.28	7.94				0.0256	0.18	0.57
0.0252	13.36	12.55	0.0156	7.87	7.56				0.0221	0.15	0.54
0.0222	13.02	12.24	0.0142	7.47	7.20				0.0196	0.12	0.52
0.0199	12.80	12.05									
0.0182	12.50	11.77									
0.0166	12.18	11.48									
0.0152	11.81	11.15									
0.0142	11.48	10.85									
0.0132	11.12	10.52									
0.0123	10.82	10.25									

Standard uncertainties: $u(\sigma) = \pm 0.02\ \mathrm{mS \cdot cm^{-1}}$, $u(T) = \pm 0.05\ \mathrm{K}$.

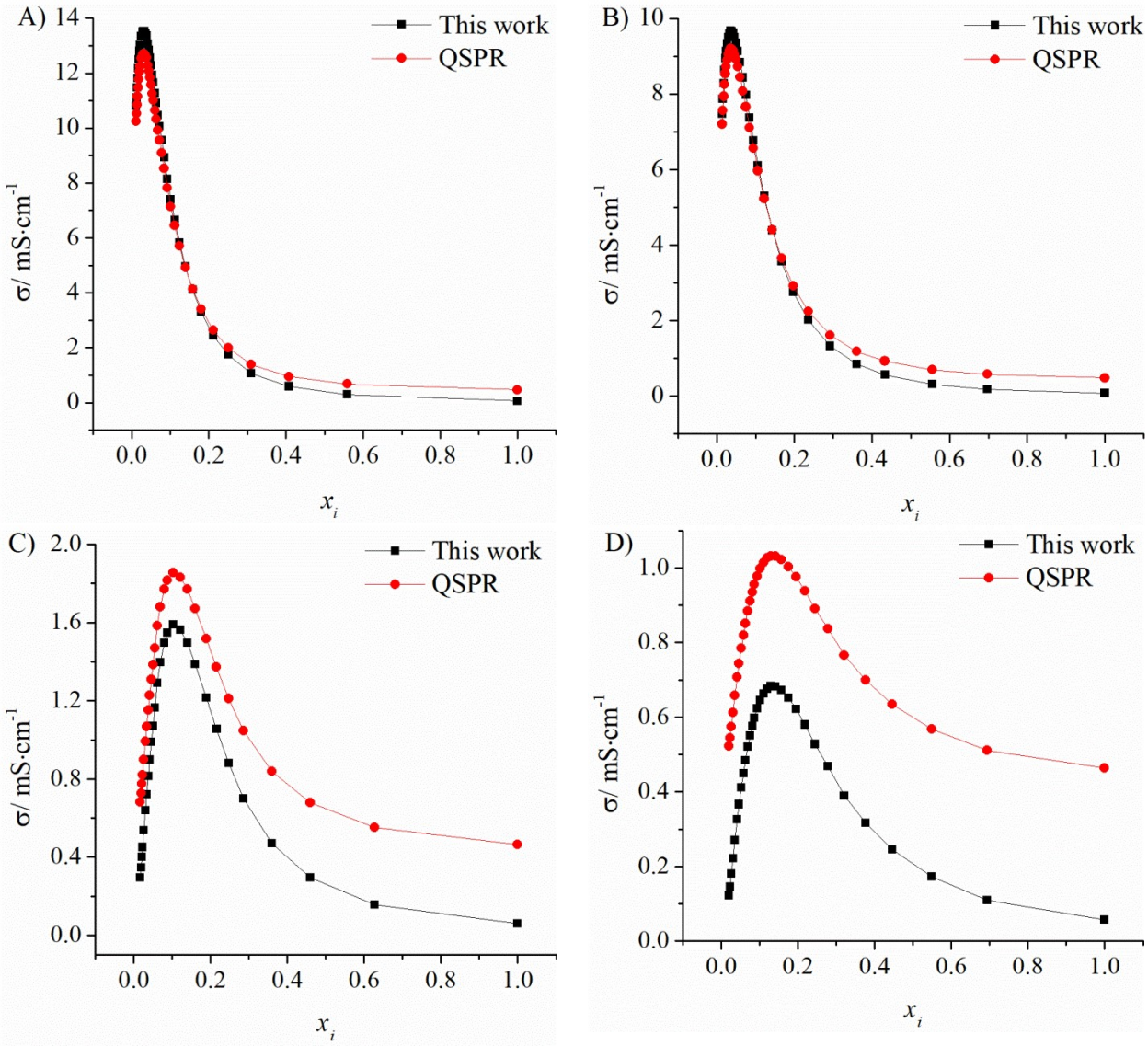

Figure S5. Comparison between experimental and calculated with QSPR model electrical conductivities of [P66614][NTf_2] binary solutions in AN (a), PC (b), DMC (c) and DEC (d).

Table S4. Electrical conductivity (σ) of [P66614][NTf_2] binary solutions in AN, PC, DMC and DEC as function of IL mole fraction (x_i) at T = (298 – 348) K.

x_i	σ/ mS·cm^{-1}										
	298 K	303 K	308 K	313 K	318 K	323 K	328 K	333 K	338 K	343 K	348 K
[P66614][NTf_2]											
This work	0.08	0.10	0.13	0.17	0.20	0.26	0.31	0.38	0.46	0.55	0.65
Ref.	0.104 [5] 0.108 [6]	0.134 [5]									
[P66614][NTf_2] + AN											
0.0200	11.46	12.08	12.73	13.37	14.03	14.72	15.38	16.05	16.75	17.46	18.16
0.0308	14.39	15.24	16.11	16.98	17.87	18.75	19.63	20.50	21.39	22.28	23.17
0.0500	12.96	13.86	14.77	15.67	16.58	17.52	18.47	19.43	20.38	21.36	22.35
0.1000	7.74	8.45	9.18	9.90	10.60	11.35	12.14	13.01	13.86	14.67	15.52
0.1500	4.80	5.35	5.92	6.51	7.08	7.65	8.23	8.82	9.47	10.15	10.87
0.2000	2.95	3.36	3.79	4.23	4.67	5.11	5.55	5.97	6.57	7.14	7.71
[P66614][NTf_2] + PN											
0.0200	9.25	9.75	10.24	10.73	11.25	11.74	12.24	12.74	13.23	13.72	14.22
0.0373	10.33	10.96	11.60	12.27	12.92	13.58	14.26	14.93	15.59	16.26	16.92
0.0500	9.96	10.62	11.31	11.98	12.69	13.42	14.13	14.84	15.56	16.28	17.00
0.1000	6.67	7.26	7.87	8.51	9.14	9.80	10.49	11.17	11.87	12.59	13.33
0.1500	3.98	4.43	4.90	5.39	5.89	6.40	6.94	7.51	8.09	8.67	9.25
0.2000	2.58	2.93	3.32	3.69	4.08	4.51	4.96	5.43	5.94	6.41	6.95
[P66614][NTf_2] + DMC											
0.0200	0.41	0.46	0.51	0.58	0.64	0.70	0.76	0.83	0.91	0.97	1.05
0.0500	1.16	1.34	1.49	1.66	1.83	2.01	2.19	2.38	2.58	2.79	2.99
0.1100	1.64	1.86	2.08	2.32	2.58	2.84	3.12	3.41	3.72	4.01	4.31
0.1500	1.43	1.63	1.83	2.07	2.30	2.57	2.84	3.11	3.42	3.71	4.04
0.2000	1.13	1.32	1.49	1.69	1.91	2.14	2.39	2.65	2.92	3.21	3.49
0.5000	0.28	0.34	0.42	0.50	0.61	0.70	0.82	0.94	1.09	1.24	1.39
[P66614][NTf_2] + DEC											
0.0200	0.13	0.15	0.17	0.19	0.21	0.24	0.26	0.27	0.30	0.33	0.35

0.0500	0.44	0.50	0.56	0.63	0.70	0.77	0.85	0.93	1.02	1.11	1.21
0.1000	0.71	0.82	0.94	1.05	1.18	1.31	1.45	1.60	1.74	1.91	2.06
0.1380	0.79	0.91	1.03	1.17	1.32	1.48	1.64	1.82	1.98	2.17	2.36
0.1500	0.75	0.86	0.99	1.12	1.27	1.42	1.59	1.76	1.93	2.13	2.33
0.2000	0.69	0.80	0.92	1.06	1.21	1.35	1.52	1.71	1.89	2.09	2.31
0.5000	0.21	0.26	0.31	0.39	0.46	0.55	0.64	0.75	0.86	0.99	1.14

Standard uncertainties: $u(\sigma) = \pm 0.02\ \mathrm{mS \cdot cm^{-1}}$, $u(T) = \pm 0.05\ \mathrm{K}$.

Table S5. Coefficients of determination (R^2) and values of parameters of the best-fit to E_a^A and A_σ^A dependencies from x with Eq. 4 – 5.

Solvents	E_a^A (Eq. 4)				A_σ^A (Eq. 5)		
	a	b	d	R^2	c	f	R^2
AN	1.88±0.26	0.12±0.03	4.7±0.5	0.9928	4.94±0.16	0.58±0.04	0.9849
PN	2.46±0.27	0.08±0.03	3.5±0.5	0.9930	4.13±0.11	0.80±0.03	0.9970
DMC	0.32±0.20	0.23±0.02	15.2±0.4	0.9945	4.95±0.17	0.62±0.04	0.9896
DEC	0.26±0.07	0.18±0.03	15.3±0.6	0.9896	4.22±0.22	0.81±0.05	0.9893

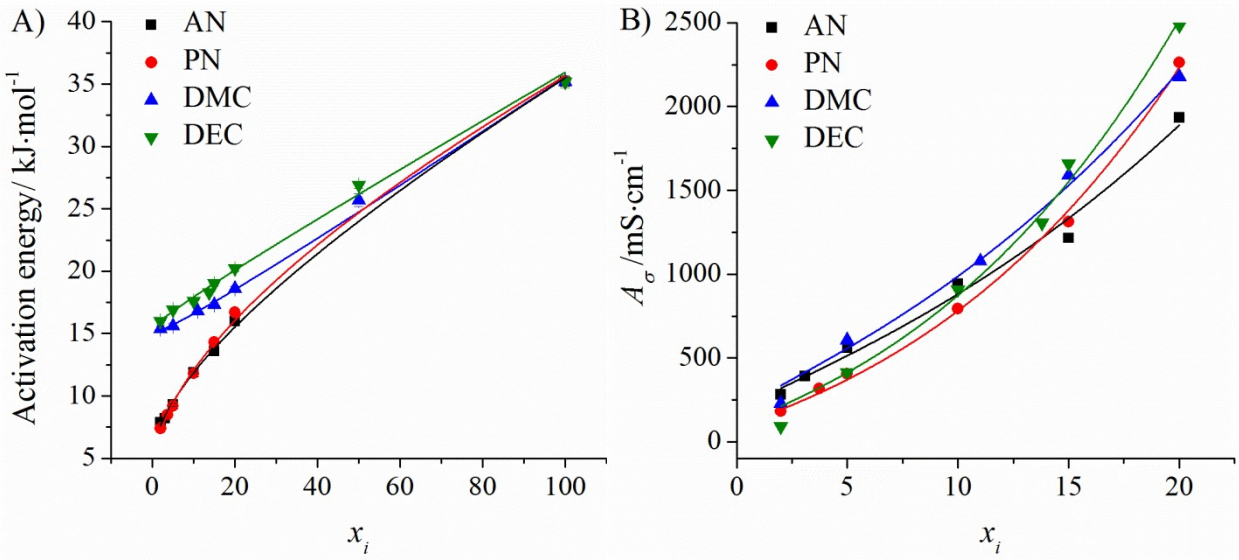

Fig. S6. Arrhenius activation energy (a) and pre-exponential factor (b) vs. mole fraction of [P66614][NTf_2] in binary solutions. Solid lines show the best fit curves.

Table S6. Experimental and literature densities of [P66614][NTf_2] binary solutions in AN, PN, DMC and DEC at atmospheric pressure in the temperature range of T = (293 – 348) K. Mole fractions of [P66614][NTf_2] in solutions correspond to their highest conductivities (see Table 2).

T/ K	ρ/ g·cm^{-3}					
	[P66614][NTf_2]		[P66614][NTf_2] + AN	[P66614][NTf_2] + PN	[P66614][NTf_2] + DMC	[P66614][NTf_2] + DEC
	This work	References				
293	1.0885	1.080[7], 1.0711[8], 1.0676[9]	0.8751	0.8683	1.0795	1.0325
298	1.0849	1.065[10], 1.070390[11], 1.0501[12]	0.8701	0.8637	1.0746	1.0279
303	1.0811	1.066774[11], 1.0483[12], 1.0603[9]	0.8649	0.8589	1.0696	1.0234
308	1.0775	1.0452[12]	0.8598	0.8543	1.0647	1.0188
313	1.0739	1.059538[11], 1.0420[12], 1.0529[9]	0.8549	0.8496	1.0599	1.0144
318	1.0700	1.0392[12]	0.8497	0.8448	1.0548	1.0097
323	1.0660	1.052297[11], 1.0356[12], 1.0457[9]	0.8443	0.8398	1.0496	1.0048
328	1.0624	1.0329[12]	0.8392	0.8351	1.0446	1.0002
333	1.0588	1.045089[11], 1.0296[12], 1.0386[9]	0.8342	0.8304	1.0398	0.9957
338	1.0555		0.8291	0.8258	1.035	0.9913
343	1.0515	1.0315[9]	0.8237	0.8207	1.0297	0.9864
348	1.0477		0.8183	0.8158	1.0245	0.9817

Standard uncertainties: $u(\rho) = \pm 1.0 \cdot 10^{-4}$ g·cm^{-3}, $u(T) = \pm 0.05$ K.

Table S7. Values of parameters of the best-fits to temperature dependencies of density of [P66614][NTf_2] solutions with Eq. (8).

	A/ g·cm^{-3}	B·10^4/ g·cm^{-3}·K^{-1}	R^2
[P66614][NTf_2]	1.3059	−7.42	0.9998
[P66614][NTf_2] + AN	1.1772	−10.15	0.9999
[P66614][NTf_2] + PN	1.1480	−9.54	0.9999
[P66614][NTf_2] + DMC	1.372	−9.98	0.9999
[P66614][NTf_2] + DEC	1.3038	−9.23	0.9999

Table S8. Isobaric thermal expansion coefficients of [P66614][NTf_2] and its AN, PC, DMC and DEC solutions calculated using Eq. (9). Mole fractions of [P66614][NTf_2] in solutions correspond to their highest conductivities (see Table 1).

T/ K	$\alpha_p \cdot 10^4$/ K^{-1}				
	[P66614][NTf_2]	[P66614][NTf_2] + AN	[P66614][NTf_2] + PN	[P66614][NTf_2] + DMC	[P66614][NTf_2] + DEC
293	6.82	11.54	10.98	9.24	8.93
298	6.84, 5.71[12]	11.60	11.05	9.29	8.97
303	6.86	11.67	11.11	9.33	9.01
308	6.89	11.74	11.17	9.37	9.05
313	6.91	11.81	11.23	9.42	9.09
318	6.93	11.88	11.29	9.46	9.14
323	6.96	11.95	11.36	9.51	9.18
328	6.98	12.02	11.42	9.55	9.22
333	7.01	12.09	11.49	9.60	9.26
338	7.03	12.17	11.56	9.65	9.31
343	7.06	12.24	11.62	9.69	9.35
348	7.08	12.32	11.69	9.74	9.39

Standard uncertainty: $u(T) = \pm 0.05$ K.

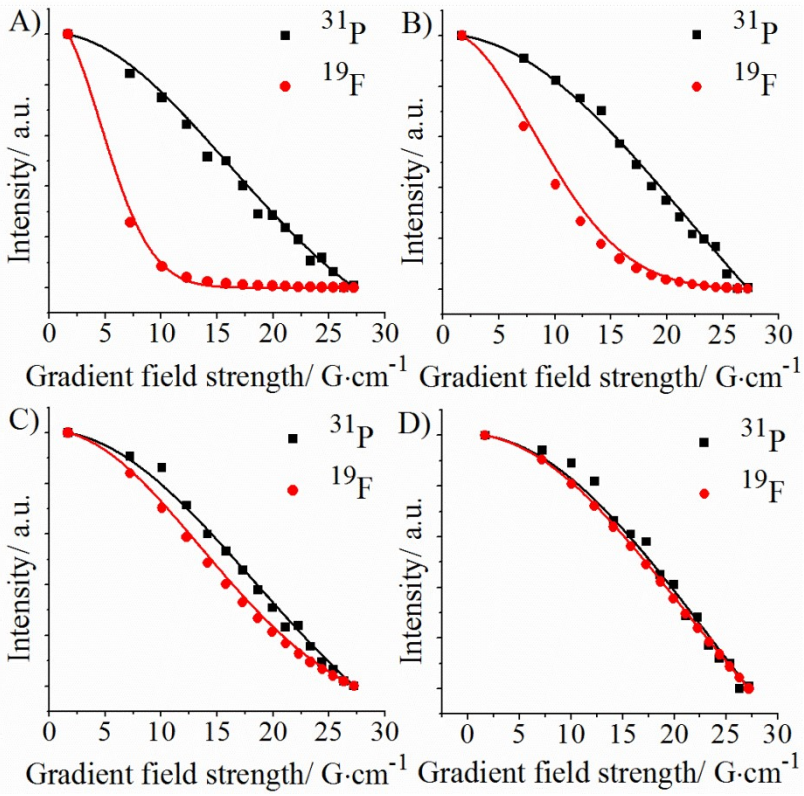

Fig. S7. NMR intensity – gradient strength plots of [P66614][NTf_2] solutions in AN (a), PN (b), DMC (c) and DEC (d). Solid lines show the best fit curves.

Table S9. Values of parameters of the best-fits to NMR intensity – gradient strength plots (Fig. S6) with Stejskal–Tanner equation $I = I_0 e^{-D\gamma^2 g^2 \delta^2 (\Delta - \frac{\delta}{3} - \frac{\tau}{2})}$.

	I_0	δ/ s	γ/ Hz·G^{-1}	Δ/ s	τ/ s
[P66614][NTf_2] + AN/ ^{19}F	12373	0.005	4005.3	0.15	0.0002
[P66614][NTf_2] + AN/ ^{31}P	11338	0.004	1723.5	0.15	0.0002
[P66614][NTf_2] + PN/ ^{19}F	12519	0.004	4005.3	0.1	0.0002
[P66614][NTf_2] + PN/ ^{31}P	12402	0.004	1723.5	0.1	0.0002
[P66614][NTf_2] + DMC/ ^{19}F	18169	0.005	4005.3	0.15	0.0002
[P66614][NTf_2] + DMC/ ^{31}P	5574	0.005	1723.5	0.5	0.0002
[P66614][NTf_2] + DEC/ ^{19}F	18437	0.005	4005.3	0.1	0.0002
[P66614][NTf_2] + DEC/ ^{31}P	11053	0.005	1723.5	0.5	0.0002

Table S10. PFG-NMR intensities of ^{19}F and ^{31}P PFG-NMR used for calculation of cation and anion diffusion coefficients in [P66614][NTf_2] solutions in AN, PN, DMC and DEC.

g/ G·cm^{-1}	[P66614][NTf_2] + AN		[P66614][NTf_2] + PN		[P66614][NTf_2] + DMC		[P66614][NTf_2] + DEC	
	$I\_^{19}F$	$I\_^{31}P$	$I\_^{19}F$	$I\_^{31}P$	$I\_^{19}F$	$I\_^{31}P$	$I\_^{19}F$	$I\_^{31}P$
1.703	11537	11273	12245	12366	18023	5549	18377	11026
7.224	3216	9974	8068	11797	15583	5213	17374	10731
10.074	1269	9177	5402	11247	13490	5045	16394	10465
12.279	764	8279	3714	10807	11710	4498	15497	10103
14.145	583	7213	2639	10496	10166	4081	14650	9310
15.791	504	7063	1968	9668	8880	3831	13861	9047
17.282	455	6249	1526	9155	7753	3555	13111	8892
18.653	417	5300	1217	8608	6790	3273	12420	8224
19.931	399	5264	1019	8266	5981	3012	11722	8031
21.131	378	4857	895	7849	5296	2731	11102	7411
22.267	355	4461	795	7418	4677	2755	10518	7375
23.348	358	3752	725	7299	4164	2449	9957	6811
24.381	330	3861	651	7107	3714	2223	9446	6559
25.371	332	3382	642	6423	3335	2118	8944	6449
26.325	333	2865	602	6057	2996	1947	8488	5946
27.245	325	2920	589	6077	2720	1877	8049	5996

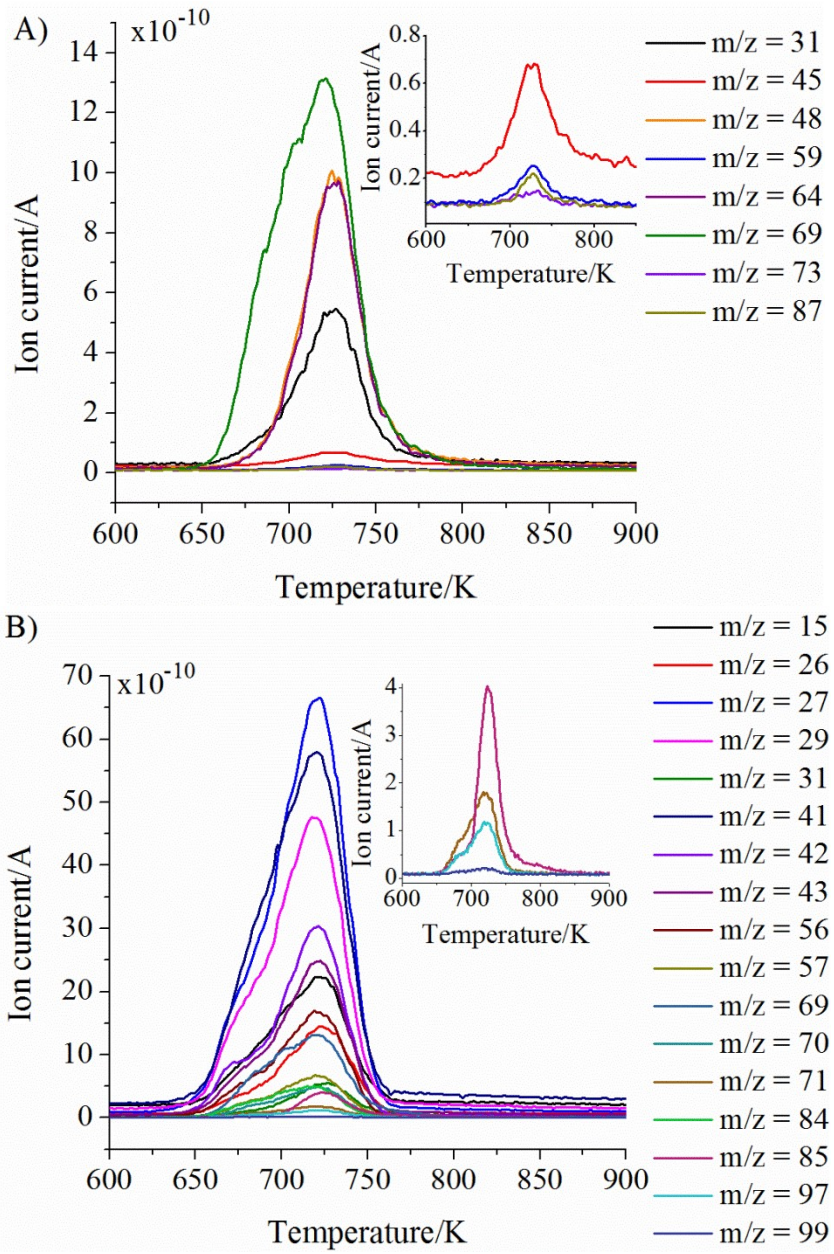

Figure S8. Ion current profiles of thermal decomposition of [P66614][NTf_2] in Ar atmosphere.

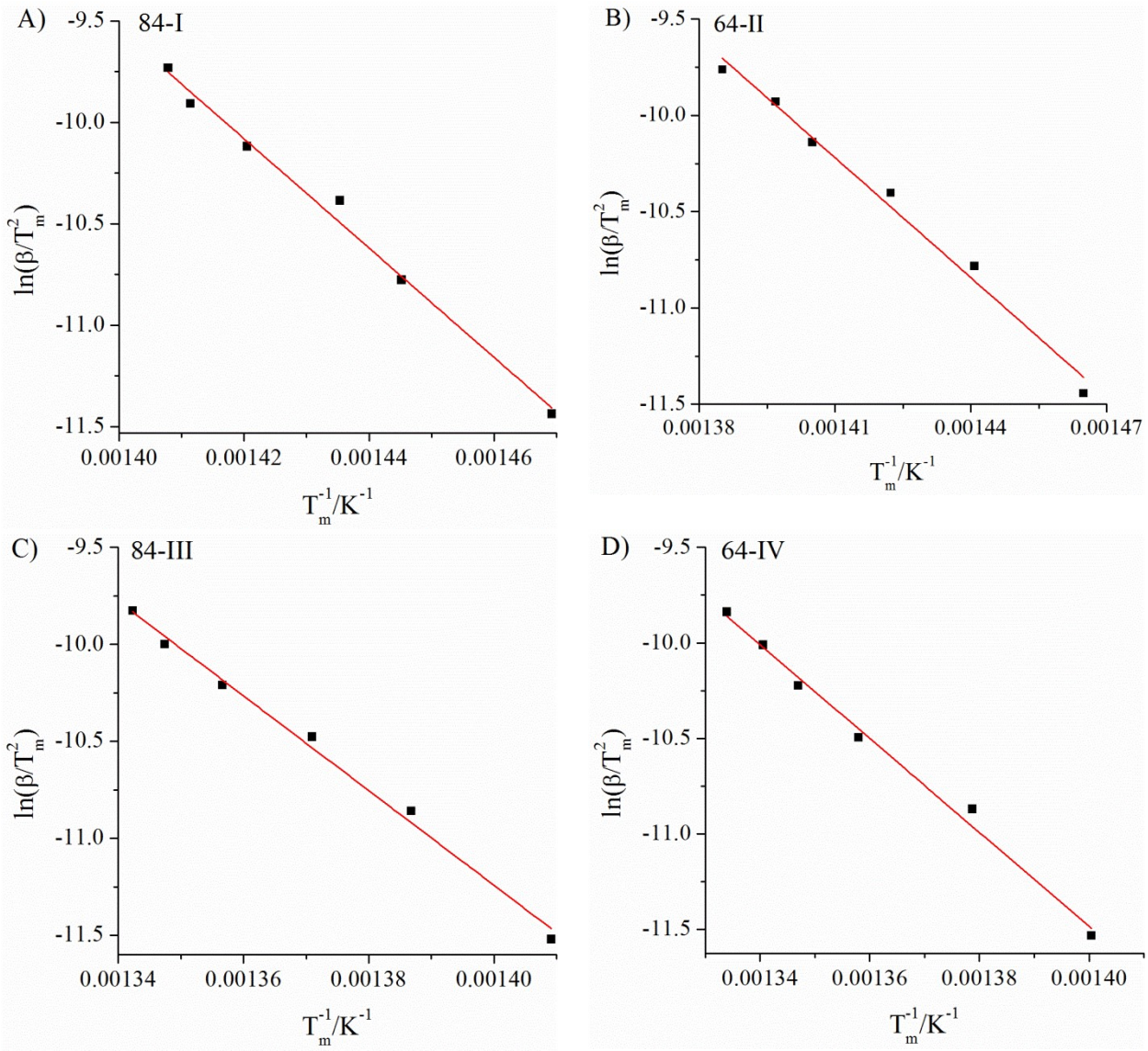

Figure S9. Kissinger plots for the decomposition of [P66614][NTf_2] in Ar atmosphere.

References

1 M. Ue, in *Encyclopedia of Electrochemical Power Sources*, Elsevier, 2009, pp. 71–84.

2 H. H. Ghazoyan, Z. L. Grigoryan, L. S. Gabrielyan and S. A. Markarian, Study of thermodynamic properties of binary mixtures of propionitrile with dimethylsulfoxide (or diethylsulfoxide) at temperatures from (298.15 to 323.15)K, *J. Mol. Liq.*, 2019, **284**, 147–156.

3 J. K. Eloranta and P. K. Kadaba, Dielectric relaxation in the mixtures of some nitriles, *Trans. Faraday Soc.*, 1970, **66**, 817–823.

4 N. A. Kermani, I. Petrushina, A. Nikiforov, J. O. Jensen and M. Rokni, Corrosion behavior of construction materials for ionic liquid hydrogen compressor, *Int. J. Hydrogen Energy*, 2016, **41**, 16688–16695.

5 A. Hernández Battez, M. Bartolomé, D. Blanco, J. L. Viesca, A. Fernández-González and R. González, Phosphonium cation-based ionic liquids as neat lubricants: Physicochemical and tribological performance, *Tribol. Int.*, 2016, **95**, 118–131.

6 R. P. Morco, J. M. Joseph and J. C. Wren, The chemical stability of phosphonium-based ionic liquids under gamma irradiation, *RSC Adv.*, 2015, **5**, 28570–28581.

7 R. E. Del Sesto, C. Corley, A. Robertson and J. S. Wilkes, Tetraalkylphosphonium-based ionic liquids, *J. Organomet. Chem.*, 2005, **690**, 2536–2542.

8 N. Rivera, A. García, R. González, A. Fernández-González, A. Hernández Battez and M. Cadenas, Ionic-liquid lubrication of a nickel-based coating reinforced with tungsten carbide particles, *J. Mol. Liq.*, 2019, **293**, 111498.

9 J. Jacquemin, R. Ge, P. Nancarrow, D. W. Rooney, M. F. Costa Gomes, A. A. H. Padua and C. Hardacre, Prediction of ionic liquid properties. I. Volumetric properties as a function of temperature at 0.1 MPa (Journal of Chemical and Engineering Data (2008) 55 (716-726)), *J. Chem. Eng. Data*, 2008, **53**, 2473.

10 G. McHale, C. Hardacre, R. Ge, N. Doy, R. W. K. Allen, J. M. MacInnes, M. R. Bown and M. I. Newton, Density-viscosity product of small-volume ionic liquid samples using quartz crystal impedance analysis, *Anal. Chem.*, 2008, **80**, 5806–5811.

11 M. Costa Gomes, L. Pison, C. Červinka and A. Padua, Porous Ionic Liquids or Liquid Metal-Organic Frameworks?, *Angew. Chemie Int. Ed.*, 2018, **57**, 11909–11912.

12 P. Kilaru, G. A. Baker and P. Scovazzo, Density and surface tension measurements of imidazolium-, quaternary phosphonium-, and ammonium-based room-temperature ionic liquids: Data and correlations, *J. Chem. Eng. Data*, 2007, **52**, 2306–2314.